LBL-24876
Preprint

Lawrence Berkeley Laboratory
UNIVERSITY OF CALIFORNIA

Materials & Chemical Sciences Division

RECEIVED
LAWRENCE
BERKELEY LABORATORY

MAY 10 1988

LIBRARY AND
DOCUMENTS SECTION

Submitted to Journal of Physical Chemistry

Explicit Approximations to the MSA for Electrolyte Systems with Unequal Ion Sizes

A.H. Harvey, T.W. Copeman, and J.M. Prausnitz

February 1988

TWO-WEEK LOAN COPY

This is a Library Circulating Copy which may be borrowed for two weeks.

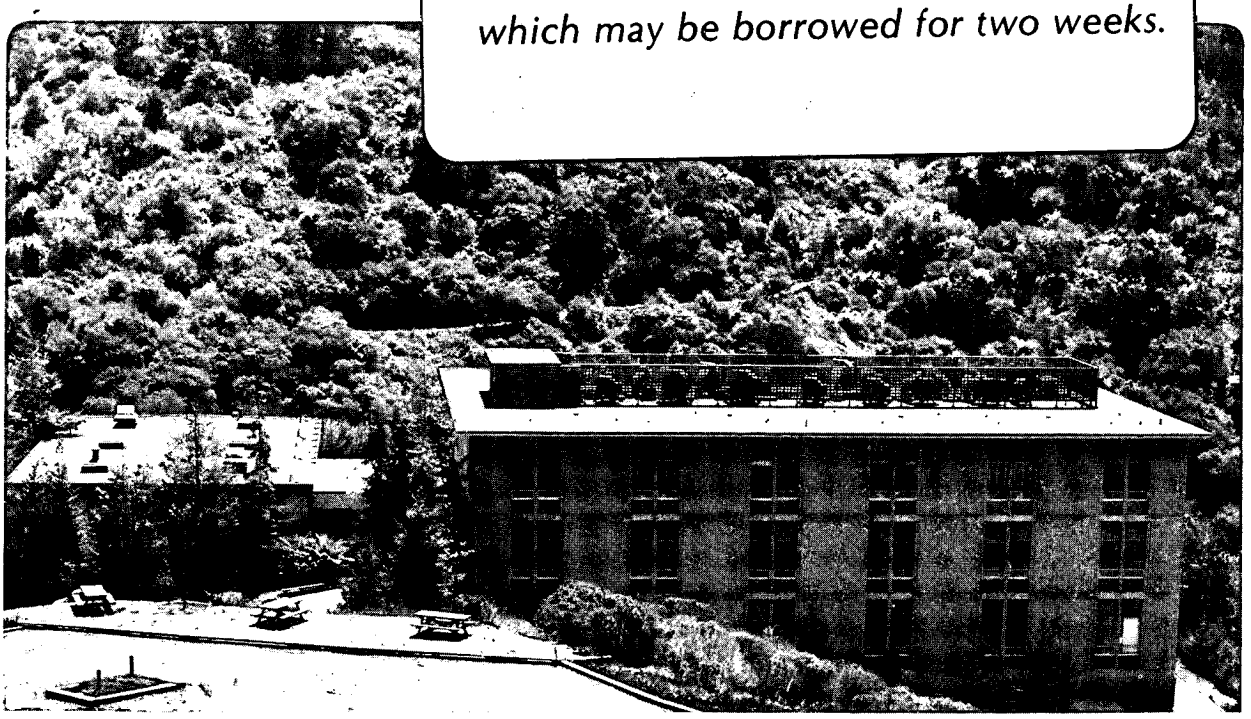

LBL-24876 c.2

Prepared for the U.S. Department of Energy under Contract DE-AC03-76SF00098

DISCLAIMER

This document was prepared as an account of work sponsored by the United States Government. While this document is believed to contain correct information, neither the United States Government nor any agency thereof, nor the Regents of the University of California, nor any of their employees, makes any warranty, express or implied, or assumes any legal responsibility for the accuracy, completeness, or usefulness of any information, apparatus, product, or process disclosed, or represents that its use would not infringe privately owned rights. Reference herein to any specific commercial product, process, or service by its trade name, trademark, manufacturer, or otherwise, does not necessarily constitute or imply its endorsement, recommendation, or favoring by the United States Government or any agency thereof, or the Regents of the University of California. The views and opinions of authors expressed herein do not necessarily state or reflect those of the United States Government or any agency thereof or the Regents of the University of California.

Explicit Approximations to the MSA for Electrolyte Systems with Unequal Ion Sizes

Allan H. Harvey
Thomas W. Copeman[†]
and
John M. Prausnitz

Materials and Chemical Sciences Division
Lawrence Berkeley Laboratory
and
Chemical Engineering Department
University of California
Berkeley, California 94720

ABSTRACT

A systematic investigation is presented for explicit approximations to the Mean Spherical Approximation (MSA) for ionic systems with ions of different size. Solution of the exact MSA for this case requires an implicit solution for the screening parameter; this complication makes it particularly undesirable for use in iterative equation-of-state calculations. This work compares with the exact MSA solution an approximation based on a linear mixing rule for a single effective ion size and a low-ion-density approximation due to Copeman and Stein. This comparison is for the electrostatic contributions to the Helmholtz energy, the pressure, and the chemical potentials; these are the quantities of primary interest in phase-equilibrium calculations using an equation of state. Over a wide range of reduced temperatures, reduced densities, and ion diameter ratios, the simple linear rule produces good results. However, for diameter ratios differing greatly from unity, better results are obtained at low ion densities from the method of Copeman and Stein. Comparison with published Monte Carlo data suggests that, when the MSA is used for the primitive model applied to aqueous electrolyte solutions, little error is introduced by the use of these approximations.

This work was supported by the Director, Office of Energy Research, Office of Basic Energy Sciences, Chemical Sciences Division of the U.S. Department of Energy under Contract No. DE-AC03-76SF00098.

[†] Air Products and Chemicals, Inc., Allentown, PA

1. Introduction

The simplest descriptions of ion-ion interactions in electrolyte solutions arise from the so-called primitive model, where the ions are modeled as charged hard spheres in a medium of uniform dielectric constant. The Mean Spherical Approximation (MSA) has been applied to the primitive model of electrolytes[1–5] and has been used by several authors to correlate activity coefficients in aqueous electrolyte solutions[6–10]. The MSA is popular, in part, because its solution, even for unequal-sized ions, is analytical. The MSA yields fair results for activity coefficients up to moderate ion concentrations, particularly if the ionic diameters are adjusted to fit the data.

However, in some vapor-liquid equilibrium (VLE) calculations, liquid-phase activity coefficients are not what one desires. Instead, it is often preferable to use a single equation of state (EOS) to compute chemical potentials (or fugacity coefficients) and pressures from the composition and density derivatives of the molar Helmholtz energy in both fluid phases. This method is particularly advantageous for mixed-solvent systems and for calculations at high pressures when the liquid phase contains supercritical components.

EOS calculations for vapor-liquid equilibria are iterative, requiring evaluation of chemical potentials and pressures at many different densities and compositions. For efficiency and reliability of these calculations, it is advantageous to use analytical (rather than numerical) derivatives of the Helmholtz energy[11]. Unfortunately, the MSA solution for systems with ions of different sizes, while analytical, is too unwieldy for efficient VLE calculations. It involves an implicit solution of a complicated equation for the screening factor; this implicit solution in particular complicates differentiation of the resulting expressions with respect to density and composition.

It is therefore desirable to find explicit approximations to the MSA which are mathematically simple yet come close to reproducing the results of the full MSA. For VLE calculations, we particularly want accurate composition derivatives (i.e. chemical potentials) and density derivatives (i.e. osmotic pressures) of the Helmholtz energy. In this work, we evaluate in a systematic manner the accuracy of two approximations: that proposed by Copeman and Stein[12,13] and a new method based on replacing the real mixture with a hypothetical mixture where the ions are of a single effective size.

Lee[14] has investigated the possibility of ignoring the P_n term (see equation (2.1) below) in the full MSA. While Lee's suggestion simplifies the equations considerably, it nevertheless requires an iterative solution for the screening factor; therefore, we did not investigate it further.

2. Explicit Approximations

For a mixture with ions of arbitrary sizes and charges, solution of the MSA yields the following equations:

$$4\Gamma^2 = \frac{\kappa^2 \sum_i \rho_i (1+\sigma_i\Gamma)^{-2} (z_i - \pi\sigma_i^2 P_n/2\Delta)^2}{\sum_i \rho_i z_i^2} \tag{2.1}$$

$$P_n = \frac{1}{\Omega}\left(\sum_j \frac{\sigma_j \rho_j z_j}{1+\sigma_j\Gamma}\right) \tag{2.1a}$$

$$\Omega = 1 + \frac{\pi}{2\Delta}\sum_j \frac{\rho_j \sigma_j^3}{1+\sigma_j\Gamma} \tag{2.1b}$$

$$\Delta = 1 - \frac{\pi}{6}\sum_j \rho_j \sigma_j^3 \tag{2.1c}$$

where $\kappa^2 = \frac{4\pi e^2}{DkT}\sum_j \rho_j z_j^2$ (κ is the reciprocal Debye screening length), e is the electronic charge, k is Boltzmann's constant, D is the static dielectric constant of the

medium, T is the absolute temperature, z_i is the valence and σ_i is the diameter of species i, ρ_i is N_i/V, the number density of species i, and the sums extend over all ionic species. Γ is the MSA screening parameter ($\Gamma \rightarrow \kappa/2$ at infinite dilution or when all $\sigma_i \rightarrow 0$) which is used in the computation of the excess thermodynamic properties (relative to a mixture of hard spheres) due to ion-ion interactions:

$$\frac{E^{ex}}{V} = -\frac{e^2}{D}\left(\Gamma \sum_i \frac{\rho_i z_i^2}{1+\sigma_i\Gamma} + \frac{\pi}{2\Delta}\Omega P_n^2\right) \tag{2.2}$$

$$\frac{A^{ex}}{V} = \frac{E^{ex}}{V} + \frac{\Gamma^3 kT}{3\pi} \tag{2.3}$$

$$\phi^{ex} = -\frac{\Gamma^3}{3\pi\sum_i \rho_i} - \frac{1}{8\sum_i \rho_i}\left(\frac{\alpha P_n}{\Delta}\right)^2 \tag{2.4}$$

$$\alpha^2 = \kappa^2 / \sum_j \rho_j z_j^2 = \frac{4\pi e^2}{DkT} \tag{2.4a}$$

$$\mu_i^{ex} = \frac{\partial(A^{ex}/V)}{\partial \rho_i} \tag{2.5}$$

where E is the internal energy, A is the Helmholtz energy, ϕ is the osmotic coefficient, and μ_i is the chemical potential (on a per-particle basis) of species i. Høye and Blum[15] present an analytical expression for μ_i^{ex} which, when the ion sizes are unequal, produces results which disagree with the derivative (2.5) (taken numerically) by an amount proportional to z_i. Since the chemical potential of an ion contains such an arbitrary constant (which depends on the choice of the zero of potential and which cancels out for an electrically-neutral combination of ions), their expression is equally correct. In this work, however, we use Equation (2.5) to be consistent with our other expressions for μ_i^{ex}.

Approximation I: Single Effective Ion Diameter

If all ions have the same diameter σ, the above equations become much simpler:

$$\Gamma = \frac{1}{2\sigma}\left[(1+2\sigma\kappa)^{1/2}-1\right] \tag{2.6}$$

$$\frac{E^{ex}}{V} = -\frac{\Gamma^3(1+\sigma\Gamma)kT}{\pi} \tag{2.7}$$

$$\frac{A^{ex}}{V} = -\frac{2\Gamma^3 kT}{3\pi}\left(1+\frac{3}{2}\sigma\Gamma\right) \tag{2.8}$$

$$\phi^{ex} = -\frac{\Gamma^3}{3\pi\sum_i \rho_i} \tag{2.9}$$

$$\frac{\mu_i^{ex}}{kT} = -\frac{\alpha^2 z_i^2}{4\pi}\frac{\Gamma}{1+\sigma\Gamma} \tag{2.10}$$

The simpler form of Equations (2.6) to (2.10) immediately suggests that it might be worthwhile to assign one effective ion size (σ_{mix}) to the mixture. A reasonable definition for σ_{mix} might be

$$\rho\sigma_{mix} = \sum_i \rho_i\sigma_i \tag{2.11}$$

where $\rho = \sum_i \rho_i$ and the sum again extends over all ionic species.

We also investigated the mixing rule

$$\rho\sigma_{mix}^3 = \sum_i \rho_i\sigma_i^3 \tag{2.12}$$

but found it to be inferior to Equation (2.11) in all cases considered.

Subsequently we refer to Equation (2.11) as Approximation I. While Equations (2.6) to (2.9) may be used directly with Equation (2.11), the composition dependence of σ_{mix} changes the expression for μ_i^{ex}:

$$\frac{\mu_i^{ex}}{kT} = -\frac{\Gamma^3}{\pi}\left[\frac{(1+\sigma_{mix}\Gamma)z_i^2}{\sum_j \rho_j z_j^2} - \frac{\Gamma}{\rho}(\sigma_i - \sigma_{mix})\right] \tag{2.13}$$

Approximation II: Low-Ion-Density Approximation

Copeman and Stein[12,13] suggested an explicit approximation, based on an

extension of the Debye-Hückel radial distribution function (and which therefore should be most accurate at the low ion densities at which Debye-Hückel theory is valid), which allows ions of different sizes. We refer to their suggestion as Approximation II. The resulting equations are:

$$4\Gamma^2 = \alpha^2 \sum_i \rho_i M_i^2 \tag{2.14}$$

$$M_i = z_i + \sigma_i \left(\frac{\pi S_{1,2}}{4\Delta} + B_i + \frac{\pi B_i S_{1,3}}{6 z_i \Delta} \right) \tag{2.14a}$$

$$B_i = -\frac{z_i \kappa}{2\left(1 + \alpha (S_{2,2})^{1/2}\right)} \tag{2.14b}$$

$$S_{m,n} = \sum_k \rho_k z_k^m \sigma_k^n \tag{2.14c}$$

$$\frac{E^{ex}}{V} = -\frac{e^2}{D} \Gamma \sum_j \frac{\rho_j z_j^2}{1 + \sigma_j \Gamma} \tag{2.15}$$

$$\frac{A^{ex}}{V} = \frac{E^{ex}}{V} + \frac{\Gamma^3 kT}{3\pi} \tag{2.3}$$

$$\phi^{ex} = -\frac{\Gamma^3}{3\pi\rho} + \frac{1}{\pi} \frac{\partial \Gamma}{\partial \rho} \left\{ \Gamma^2 - \frac{\alpha^2}{4} \left[\sum_i \frac{\rho_i z_i^2}{1+\sigma_i \Gamma} - \Gamma \sum_i \frac{\rho_i z_i^2 \sigma_i}{(1+\sigma_i \Gamma)^2} \right] \right\} \tag{2.16}$$

$$\frac{\partial \Gamma}{\partial \rho} = \frac{\Gamma}{2\rho} + \frac{\pi \alpha^2}{8 \Delta^2 \Gamma \rho} \sum_i \rho_i \sigma_i M_i \left[\frac{B_i S_{1,3}}{3 z_i} + \frac{S_{1,2}}{2} + \frac{B_i \Delta}{1 + \alpha (S_{2,2})^{1/2}} \left(\frac{S_{1,3}}{6 z_i} + \frac{\Delta}{\pi} \right) \right] \tag{2.16a}$$

$$\frac{\mu_i^{ex}}{kT} = \frac{\Gamma^2}{\pi} \frac{\partial \Gamma}{\partial \rho_i} - \frac{\alpha^2}{4\pi} \left[\frac{z_i^2 \Gamma}{1+\sigma_i \Gamma} + \sum_j \frac{\rho_j z_j^2 \frac{\partial \Gamma}{\partial \rho_i}}{(1+\sigma_j \Gamma)^2} \right] \tag{2.17}$$

$$\frac{\partial \Gamma}{\partial \rho_i} = \frac{\alpha^2}{8\Gamma} \left\{ M_i^2 + 2 \sum_j \rho_j \sigma_j M_j \left[\frac{\pi \sigma_i^2}{4\Delta^2} \left(z_i \Delta + \frac{\pi}{6} \sigma_i S_{1,2} \right) + \frac{\partial B_j}{\partial \rho_i} \right. \right. \tag{2.17a}$$

$$\left. \left. + \frac{\pi}{6 z_j \Delta^2} \left(\left(\frac{\partial B_j}{\partial \rho_i} S_{1,3} + z_i \sigma_i^3 B_j \right) \Delta + \frac{\pi}{6} \sigma_i^3 B_j S_{1,3} \right) \right] \right\}$$

$$\frac{\partial B_j}{\partial \rho_i} = \frac{B_j z_i^2}{2}\left[\frac{1}{S_{2,0}} - \frac{\alpha\sigma_i^2 (S_{2,2})^{-1/2}}{1+\alpha(S_{2,2})^{1/2}}\right] \tag{2.17b}$$

The equations for the excess osmotic coefficient and chemical potentials are newly derived in this work and may not be in the most concise form possible. Equation (2.3) replaces the approximate Helmholtz energy function given previously[13].

3. Comparison of Approximations

To ascertain the accuracy of Approximations I and II, we examine results for excess Helmholtz energy A^{ex}, excess osmotic coefficient ϕ^{ex}, and excess chemical potentials μ_i^{ex}; these are the quantities especially relevant for EOS calculations.

To make a systematic comparison, we restrict attention to a system containing only one cationic species (with diameter σ_+ and charge +|z|) and one anionic species (with diameter σ_- and charge -|z|). This system can be completely characterized by a dimensionless reciprocal temperature, dimensionless density, and diameter ratio:

$$\beta^* = \frac{|z|^2 e^2}{DkT\bar{\sigma}} \tag{3.1}$$

$$\rho^* = \rho\bar{\sigma}^3 \tag{3.2}$$

$$r = \frac{\sigma_+}{\sigma_-} \tag{3.3}$$

where $\bar{\sigma} = \frac{1}{2}(\sigma_+ + \sigma_-)$.

To interpret the results, we define a dimensionless screening factor, internal energy, Helmholtz energy, and chemical potential (the osmotic coefficient is already dimensionless):

$$\Gamma^* = \Gamma\bar{\sigma} \tag{3.4}$$

$$E^{*ex} = \frac{E^{ex}}{NkT} \tag{3.5}$$

$$A^{*ex} = \frac{A^{ex}}{NkT} \tag{3.6}$$

$$\mu_i^{*ex} = \frac{\mu_i^{ex}}{kT} \tag{3.7}$$

Using these reduced variables, dimensionless equations may be obtained which are analogous to Equations (2.1) to (2.5) for the full MSA; to Equations (2.6) to (2.9) and (2.13) for Approximation I; and to Equations (2.14) to (2.17) for Approximation II. These equations are given in the Appendix.

We note that these properties are not all independent. In the primitive model, we have the following thermodynamic identity:

$$\frac{A^{ex}}{V} = \sum_i \rho_i \mu_i^{ex} - \frac{\rho}{\beta}\phi^{ex} \tag{3.8}$$

For our test case in dimensionless form, this becomes

$$A^{*ex} = \tfrac{1}{2}(\mu_+^{*ex} + \mu_-^{*ex}) - \phi^{ex} \tag{3.9}$$

Equation (3.9) was used to verify the internal consistency of our calculations.

Our systematic analysis of Approximations I and II consists of determining, for fixed values of r (0.25, 0.50, and 0.75), the region in the (ρ^*, β^*) plane wherein each approximation is accurate to within 1%, 2%, 5%, 10%, and 25% of the full MSA result for A^{*ex}, ϕ^{ex}, μ_+^{*ex}, and μ_-^{*ex}. These were made into contour plots for the physically-interesting portion of the (ρ^*, β^*) plane: ρ^* up to 1 and β^* from 1 to 100. (Comparison with the MSA is, however, less meaningful at high β^* and low ρ^* because the MSA is a poor approximation in this region, as discussed in Section 4.) The aqueous electrolyte regime is characterized by β^* near 2 (for 1-1 electrolytes) and ρ^* up to approximately 0.2. A typical molten salt would have β^* near 50 and ρ^* near 0.7. As a specific example, a one-molar solution of sodium chloride in water at 25°C would have (using Pauling crystal diameters for the ions)

$\rho^* = 0.0253$, $\beta^* = 2.59$, and r = 0.525. Molten sodium chloride at its melting temperature (1074 K) has $\rho^* = 0.672$, $\beta^* = 56.5$.

Figures 1-4 show combined contour plots for the two approximations for an ion size ratio of 0.5. The solid contours show the error in Approximation I, the dashed contours are for Approximation II, and the shading indicates the region where the result from Approximation II comes closer to reproducing the result from the full MSA. For clarity, the 2% contour is omitted from Figure 3; this graph (for the chemical potential of the small ion) is complicated because, for both approximations, the error changes sign, producing two contours for each magnitude of the error.

The following conclusions can be drawn from Figures 1-4:

1) Approximation II is generally better than Approximation I at low densities for all properties except μ_+^{*ex}, where it is better at high β^* and only slightly worse at low β^*.

2) As the density increases, Approximation I gets worse slowly, but the error in Approximation II increases drastically. The latter is to be expected, as Approximation II is based on a Debye-Hückel radial distribution function.

3) Both approximations get worse at high β^*; the errors (at constant ρ^*) tend to go through a minimum at β^* somewhere between 2 and 10. Fortunately, this region of minimum error lies roughly in the aqueous electrolyte regime.

4) Though both approximations give very good results for the excess Helmholtz energy in the aqueous electrolyte regime, the errors in the derivative properties (osmotic coefficient and chemical potentials) in this region tend to be two or three times as high as those in A^{*ex}.

5) Neither approximation performs well in the molten-salt region; Approximation

II is particularly unsuitable at these conditions.

A remaining factor to consider is the influence of the ion size ratio. Figures 5 and 6 are contour plots for ϕ^{ex} at ratios of 0.25 and 0.75, respectively. In conjunction with Figure 2, these show the effect of the size ratio on the errors in ϕ^{ex}. The effect on the contour plots for the other properties is similar; the rest of the plots at r = 0.25 and r = 0.75 are shown in Figures 7-12.

As expected, the size ratio has a large influence on the accuracy of Approximation I, which becomes exact when r = 1. Approximation II also gets worse as the size ratio deviates from unity, but the effect is not as severe.

Finally, we note that Blum[16] has recently presented an examination of the choice of the effective ion size σ_{mix} to be used in solving for the screening factor via Equation (2.6). His $\Gamma \rightarrow 0$ limit approaches our Approximation I as $\rho \rightarrow 0$ when all $|z_i|$ are equal. An interesting point raised by Blum's work is the influence of the ionic charges on the optimum σ_{mix}. His results suggest to us that, for systems with ions of differing charge, a simple improvement to Approximation I might be given by

$$\bar{\sigma} = \sum_i \rho_i \sigma_i z_i^2 \,/\, \sum_i \rho_i z_i^2 \tag{3.10}$$

Because our test system requires the charges on the two species to be equal and opposite (otherwise a fourth dimensionless group would be required), our results do not address the effect of unequal charges on the accuracy of explicit approximations to the MSA. This question is probably worthy of further study. We point out, however, that Approximation I is equivalent to the full MSA for equal-sized ions regardless of their charges.

4. Comparison with Monte Carlo Results

A limited amount of computer-simulation data is available for the primitive

model for unequal-sized ions. We compare our calculations to Monte Carlo data of Abramo, et al.[17] for 1-1 aqueous electrolytes and to Monte Carlo data of Rogde[18] for 2-2 aqueous electrolytes. Both studies report internal energies and osmotic coefficients; we found no published data for Helmholtz energies or chemical potentials for systems with unequal ion sizes.

Table I (for Abramo's data) and Table II (for Rogde's data) present the Monte Carlo results for excess internal energies and excess osmotic coefficients along with the corresponding values calculated from the full MSA and from the two explicit approximations. The reported Monte Carlo values for the osmotic coefficient included the hard-sphere contribution; ϕ^{ex} was obtained by subtracting out PV/NkT for the hard-sphere mixture as given by the equation of Mansoori, et al.[19].

We see from Tables I and II that even the full MSA does not always yield highly accurate results for the primitive model; this is especially true at higher β^* (2-2 aqueous electrolytes). The differences between the thermodynamic properties calculated from the explicit approximations and those calculated from the MSA are often smaller in magnitude than the deviation of the MSA from the Monte Carlo results. As expected, this result is especially valid for those regions where the explicit approximations work well, i.e. for Approximation I with r near unity and for Approximation II at low densities.

Monte Carlo studies in the restricted primitive model (equal ion sizes) also show that the MSA is a poor approximation to the primitive model at high β^* and low ρ^* because behavior at these conditions is dominated by ion pairing and clustering[20,21]. Corrections to the MSA have been considered for the equal-sized case[22,23]; these could be used in conjunction with Equation (2.11) to improve Approximation I at conditions where the MSA is inadequate.

5. Conclusions

We have investigated two explicit approximations to the MSA for thermodynamic properties in the primitive model of ionic systems. For conditions typical of aqueous electrolytes, Approximation I is satisfactory, particularly if the ion-size ratio is not less than 0.5. At low concentrations, Approximation II is better, but it quickly becomes unsuitable at high concentrations. Based on comparison with a limited amount of Monte Carlo data, these approximations, for primitive-model conditions characteristic of most aqueous electrolyte solutions, introduce only errors which are no larger than those introduced by the MSA itself. Such approximation is therefore justified for practical calculations where analytical differentiation is desirable or where computational efficiency is important.

6. Acknowledgements

This work was supported by the Director, Office of Energy Research, Office of Basic Energy Sciences, Chemical Sciences Division of the U.S. Department of Energy under Contract No. DE-AC03-76SF00098. The authors thank Professor K.S. Pitzer for helpful discussions and Professor L. Blum for helpful correspondence and for sending a preprint of his work.

REFERENCES

(1) Waisman, E.; Lebowitz, J.L. *J. Chem. Phys.*, **1970**, *52*, 4307.

(2) Waisman, E.; Lebowitz, J.L. *J. Chem. Phys.*, **1972**, *56*, 3086, 3093.

(3) Blum, L. *Mol. Phys.*, **1975**, *30*, 1529.

(4) Blum, L. *Theoretical Chemistry: Advances and Perspectives*, **1980**, *5*, 1.

(5) Blum, L.; Høye, J.S. *J. Phys. Chem.*, **1977**, *81*, 1311.

(6) Triolo, R.; Grigera, J.R.; Blum, L. *J. Phys. Chem.*, **1976**, *80*, 1858.

(7) Triolo, R.; Blum, L.; Floriano, M. *J. Chem. Phys.*, **1978**, *67*, 5956.

(8) Watanasiri, S.; Brulé, M.R.; Lee, L.L. *J. Phys. Chem.*, **1982**, *86*, 292.

(9) Ball, F.-X.; Planche, H.; Fürst, W.; Renon, H. *AIChE Journal*, **1985**, *31*, 1233.

(10) Corti, H.R. *J. Phys. Chem.*, **1987**, *91*, 686.

(11) Topliss, R.J., PhD Dissertation, University of California, Berkeley (1985).

(12) Copeman, T.W.; Stein, F.P. *Fluid Phase Equilibria*, **1986**, *30*, 237.

(13) Copeman, T.W.; Stein, F.P. *Fluid Phase Equilibria*, **1987**, *35*, 165.

(14) Lee, L.L. *J. Chem. Phys.*, **1983**, *78*, 5270.

(15) Høye, J.S.; Blum, L. *Mol. Phys.*, **1978**, *35*, 299.

(16) Blum, L., preprint (1987).

(17) Abramo, M.C.; Caccamo, C.; Malescio, G.; Pizzimenti, G.; Rogde, S.A. *J. Chem. Phys.*, **1984**, *80*, 4396.

(18) Rogde, S.A. *Chem. Phys. Lett.*, **1983**, *103*, 133.

(19) Mansoori, G.A.; Carnahan, N.F.; Starling, K.E.; Leland, T.W. *J. Chem. Phys.*, **1971**, *54*, 1523.

(20) Valleau, J.P.; Cohen, L.K.; Card, D.N. *J. Chem. Phys.*, **1980**, *72*, 5942.

(21) Pitzer, K.S.; Schreiber, D.R. *Mol. Phys.*, **1987**, *60*, 1067.

(22) Stell, G.; Larsen, B. *J. Chem. Phys.*, **1979**, *70*, 361.

(23) Henderson, D. *ACS Adv. in Chem. Ser.*, **1983**, No. 204, 47.

APPENDIX

Dimensionless Equations for the Screening Factor, Internal Energy, Helmholtz Energy, Osmotic Coefficient, and Single-Ion Chemical Potentials

It is convenient to define the following dimensionless parameters in addition to those defined in Section 3:

$$\xi_+ = \frac{\sigma_+}{\bar{\sigma}} = \frac{2r}{r+1} \tag{A.1}$$

$$\xi_- = \frac{\sigma_-}{\bar{\sigma}} = \frac{2}{r+1} \tag{A.2}$$

$$\kappa^* = \kappa\bar{\sigma} = (4\pi\beta^*\rho^*)^{1/2} \tag{A.3}$$

$$\alpha^* = \alpha|z|/\bar{\sigma}^{1/2} = \kappa^*/\rho^{*1/2} \tag{A.4}$$

$$\rho_i^* = \rho_i\bar{\sigma}^3 \tag{A.5}$$

$$P_n^* = \bar{\sigma}^2 P_n/|z| \tag{A.6}$$

$$B_j^* = \bar{\sigma}B_j/|z| \tag{A.7}$$

$$M_i^* = M_i/|z| \tag{A.8}$$

$$S_{m,n}^* = S_{m,n}\bar{\sigma}^{(3-n)}/|z|^m \tag{A.9}$$

$$\Gamma_\rho^* = \bar{\sigma}^{-2}\frac{\partial\Gamma}{\partial\rho} \tag{A.10}$$

For the model described in Section 3, the screening factor and the electrostatic contributions to the internal energy, Helmholtz energy, osmotic coefficient, and ionic chemical potentials are given as follows:

Full MSA

$$\Gamma^{*2} = \frac{\kappa^{*2}}{8}\left[(1+\xi_+\Gamma^*)^{-2}\left(1-\frac{\pi\xi_+^2P_n^*}{2\Delta}\right)^2 + (1+\xi_-\Gamma^*)^{-2}\left(-1-\frac{\pi\xi_-^2P_n^*}{2\Delta}\right)^2\right] \tag{A.11}$$

$$P_n^* = \frac{\rho^*}{2\Omega}\left(\frac{\xi_+}{1+\xi_+\Gamma^*} - \frac{\xi_-}{1+\xi_-\Gamma^*}\right) \tag{A.11a}$$

$$\Omega = 1 + \frac{\pi\rho^*}{4\Delta}\left(\frac{\xi_+^3}{1+\xi_+\Gamma^*} + \frac{\xi_-^3}{1+\xi_-\Gamma^*}\right) \tag{A.11b}$$

$$\Delta = 1 - \frac{\pi}{12}\rho^* \left(\xi_+^3 + \xi_-^3\right) \tag{A.11c}$$

$$E^{*\alpha} = -\beta^* \left[\frac{\Gamma^*}{2}\left(\frac{1}{1+\xi^+\Gamma^*} + \frac{1}{1+\xi_-\Gamma^*}\right) + \frac{\pi}{2\Delta\rho^*}\Omega P_n^{*2}\right] \tag{A.12}$$

$$A^{*\alpha} = E^{*\alpha} + \frac{\Gamma^{*3}}{3\pi\rho^*} \tag{A.13}$$

$$\phi^{\alpha} = -\frac{\Gamma^{*3}}{3\pi\rho^*} - \frac{\kappa^{*2}P_n^{*2}}{8\Delta^2\rho^{*2}} \tag{A.14}$$

$$\mu_\pm^{*\alpha} = \frac{\partial(\rho^* A^{*\alpha})}{\partial\rho_\pm^*} \tag{A.15}$$

Approximation I

$$\Gamma^* = ½\left((1+2\kappa^*)^{½} - 1\right) \tag{A.16}$$

$$E^{*\alpha} = -\frac{\Gamma^{*3}(1+\Gamma^*)}{\pi\rho^*} \tag{A.17}$$

$$A^{*ex} = -\frac{2\Gamma^{*3}(1+\frac{3}{2}\Gamma^*)}{3\pi\rho^*} \tag{A.18}$$

$$\phi^{\alpha} = -\frac{\Gamma^{*3}}{3\pi\rho^*} \tag{A.19}$$

$$\mu_\pm^{*ex} = -\frac{\Gamma^{*3}}{\pi\rho^*}\left[1+\Gamma^*(2-\xi_\pm)\right] \tag{A.20}$$

Approximation II

$$\Gamma^{*2} = \frac{\kappa^{*2}}{8}\left(M_+^{*2} + M_-^{*2}\right) \tag{A.21}$$

$$M_\pm^* = \pm 1 + \xi_\pm\left(\frac{\pi S_{1,2}^*}{4\Delta} + B_\pm^* \pm \frac{\pi B_\pm^* S_{1,3}^*}{6\Delta}\right) \tag{A.21a}$$

$$B_\pm^* = \pm\frac{-\kappa^*}{2(1+\alpha^*(S_{2,2}^*)^{½})} \tag{A.21b}$$

$$S_{m,n}^* = \frac{\rho^*}{2}\left(\xi_+^n + (-1)^m\xi_-^n\right) \tag{A.21c}$$

$$E^{*\alpha} = -½\beta^*\Gamma^*\left(\frac{1}{1+\xi_+\Gamma^*} + \frac{1}{1+\xi_-\Gamma^*}\right) \tag{A.22}$$

$$A^{*\alpha} = E^{*\alpha} + \frac{\Gamma^{*3}}{3\pi\rho^*} \tag{A.13}$$

$$\phi^{ex} = -\frac{\Gamma^{*3}}{3\pi\rho^*} + \frac{\Gamma_\rho^*}{\pi}\left\{\Gamma^{*2} - \frac{\kappa^{*2}}{8}\left[\left(\frac{1}{1+\xi_+\Gamma^*} + \frac{1}{1+\xi_-\Gamma^*}\right) - \Gamma^*\left(\frac{\xi_+}{(1+\xi_+\Gamma^*)^2} + \frac{\xi_-}{(1+\xi_-\Gamma^*)^2}\right)\right]\right\} \quad \text{(A.23)}$$

$$\Gamma_\rho^* = \frac{\Gamma^*}{2\rho^*} + \frac{\pi\alpha^{*2}}{16\Delta^2\Gamma^*}(\xi_+ M_+^* R_+^* + \xi_- M_-^* R_-^*) \quad \text{(A.23a)}$$

$$R_\pm^* = \frac{S_{1,2}^*}{2} \pm \frac{B_\pm^* S_{1,3}^*}{3} + \frac{B_\pm^*\Delta}{1+\alpha^*(S_{2,2}^*)^{1/2}}\left(\frac{\Delta}{\pi} \pm \frac{S_{1,3}^*}{6}\right) \quad \text{(A.23b)}$$

$$\mu_\pm^{*ex} = \beta^*\left\{\frac{-\Gamma^*}{1+\xi_\pm\Gamma^*} + \left[M_\pm^{*2} + \frac{\rho^*}{\Delta^2}(\xi_+ M_+^* C_{\pm,+}^* + \xi_- M_-^* C_{\pm,-}^*)\right]\left[\frac{\Gamma^*}{2} - \frac{\kappa^{*2}}{16\Gamma^*}\left(\frac{1}{(1+\xi_+\Gamma^*)^2} + \frac{1}{(1+\xi_-\Gamma^*)^2}\right)\right]\right\} \quad \text{(A.24)}$$

$$C_{+,\pm}^* = B_\pm^*\left\{L_+^*\Delta^2 \pm \frac{\pi}{6}\left[(L_+^* S_{1,3}^* + \xi_+^3)\Delta + \frac{\pi}{6}\xi_+^3 S_{1,3}^*\right]\right\} + \frac{\pi\xi_+^2}{4}\left(\frac{\pi}{6}\xi_+ S_{1,2}^* + \Delta\right) \quad \text{(A.24a)}$$

$$C_{-,\pm}^* = B_\pm^*\left\{L_-^*\Delta^2 \pm \frac{\pi}{6}\left[(L_-^* S_{1,3}^* - \xi_-^3)\Delta + \frac{\pi}{6}\xi_-^3 S_{1,3}^*\right]\right\} + \frac{\pi\xi_-^2}{4}\left(\frac{\pi}{6}\xi_- S_{1,2}^* - \Delta\right) \quad \text{(A.24b)}$$

$$L_\pm^* = \frac{1}{2\rho^*} - \frac{\xi_\pm^2\alpha^*(S_{2,2}^*)^{-1/2}}{2\left(1+\alpha^*(S_{2,2}^*)^{1/2}\right)} \quad \text{(A.24c)}$$

Table I. Comparison of Approximations I and II and Full MSA to Monte Carlo Data for Excess Internal Energy and for Excess Osmotic Coefficient for 1-1 Aqueous Electrolytes.

ρ^*	β^*	r	$-E^{*\alpha}$				$-\phi^{\alpha}$			
			MC	MSA	I	II	MC	MSA	I	II
.12800	1.888	0.8	.690±.002	.6793	.6771	.7075	.142±.014	.1459	.1448	.1408
.08990	2.124	0.6	.734±.003	.7305	.7196	.7597	.157±.010	.1641	.1586	.1575
.06023	2.428	0.4	.789±.002	.7999	.7686	.8312	.184±.007	.1913	.1751	.1808
.02921	3.090	0.1	.893±.002	.9703	.8584	.9955	.215±.006	.2674	.2066	.2473
.06506	1.888	0.8	.581±.002	.5724	.5710	.5872	.136±.007	.1336	.1328	.1318
.04569	2.124	0.6	.613±.002	.6093	.6023	.6237	.146±.005	.1477	.1438	.1449
.03061	2.428	0.4	.657±.002	.6572	.6378	.6712	.166±.003	.1677	.1567	.1625
.02765	1.888	0.8	.455±.002	.4469	.4461	.4526	.113±.003	.1141	.1136	.1136
.01942	2.124	0.6	.475±.001	.4698	.4661	.4748	.121±.002	.1236	.1213	.1224
.01301	2.428	0.4	.507±.002	.4981	.4882	.5020	.132±.003	.1362	.1300	.1334
.00651	1.888	0.8	.283±.001	.2721	.2719	.2728	.079±.001	.0777	.0776	.0776
.00457	2.124	0.6	.295±.001	.2808	.2797	.2812	.084±.001	.0817	.0810	.0813
.00306	2.428	0.4	.307±.001	.2908	.2882	.2907	.088±.001	.0866	.0847	.0855
.02532	2.588	0.525	.677±.004	.6646	.6550	.6763	.166±.004	.1686	.1631	.1658
.01013	2.588	0.525	.511±.003	.4932	.4886	.4964	.135±.002	.1350	.1321	.1337
.00253	2.588	0.525	.316±.002	.2934	.2922	.2936	.091±.001	.0873	.0864	.0868
.01686	2.963	0.275	.725±.003	.7209	.6912	.7314	.183±.003	.1941	.1766	.1875
.00674	2.963	0.275	.546±.002	.5230	.5093	.5246	.143±.002	.1493	.1406	.1458
.00169	2.963	0.275	.332±.002	.3035	.2999	.3028	.094±.001	.0924	.0899	.0911

Table II. Comparison of Approximations I and II and Full MSA to Monte Carlo Data for Excess Internal Energy and for Excess Osmotic Coefficient for 2-2 Aqueous Electrolytes.

ρ^*	β^*	r	$-E^{*\alpha}$				$-\phi^{\alpha}$			
			MC	MSA	I	II	MC	MSA	I	II
.13011	7.573	0.8	3.744±.011	3.640	3.624	3.948	.67±.03	.636	.630	.519
.09138	8.519	0.6	4.089±.012	3.991	3.906	4.327	.71±.03	.737	.705	.612
.06122	9.736	0.4	4.588±.018	4.504	4.242	4.896	.77±.02	.901	.798	.756
.06506	7.573	0.8	3.359±.010	3.188	3.176	3.384	.63±.02	.619	.615	.569
.04569	8.519	0.6	3.718±.012	3.460	3.401	3.666	.66±.02	.706	.681	.654
.03061	9.736	0.4	4.235±.017	3.841	3.664	4.070	.67±.07	.838	.762	.780
.02602	7.573	0.8	2.923±.012	2.592	2.583	2.685	.46±.05	.571	.568	.557
.01828	8.519	0.6	3.280±.013	2.775	2.741	2.868	.54±.04	.635	.620	.622
.01224	9.736	0.4	3.831±.018	3.016	2.920	3.113	.55±.08	.727	.681	.711
.00651	7.573	0.8	2.331±.012	1.760	1.757	1.781	.43±.03	.451	.450	.450
.00457	8.519	0.6	2.723±.014	1.846	1.834	1.866	.46±.05	.486	.480	.484
.00306	9.736	0.4	3.322±.020	1.951	1.920	1.969	.50±.08	.530	.514	.527

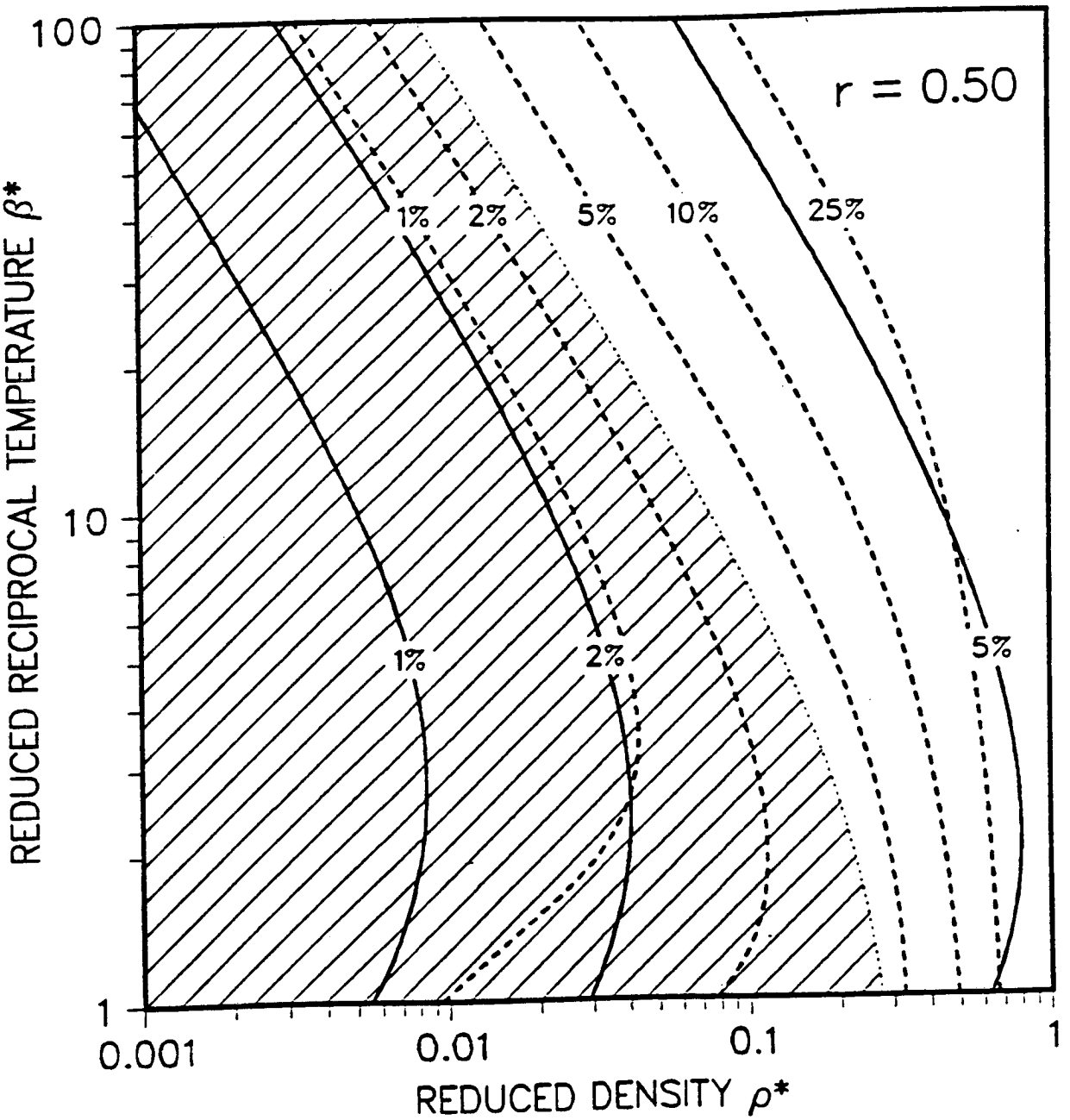

Figure 1: Contour Plot for Deviation from Full MSA Results for A^{*ex} at r = 0.50. Solid Lines for Approximation I; Dashed Lines for Approximation II. Shading Indicates Region where Error from Approximation II is Smaller.

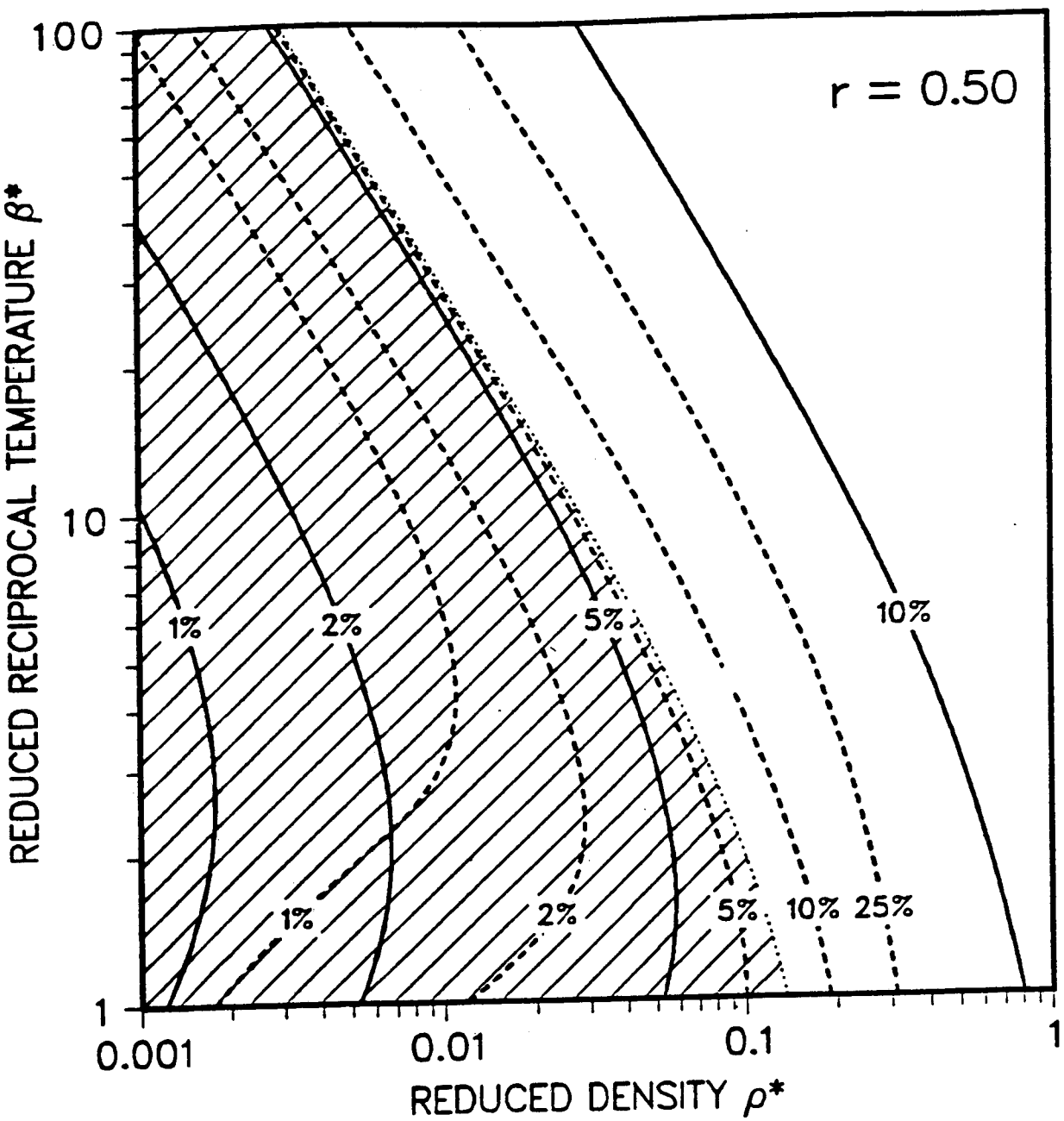

Figure 2: Contour Plot for Deviation from Full MSA Results for ϕ^{ex} at r = 0.50. Lines and Shading as in Figure 1.

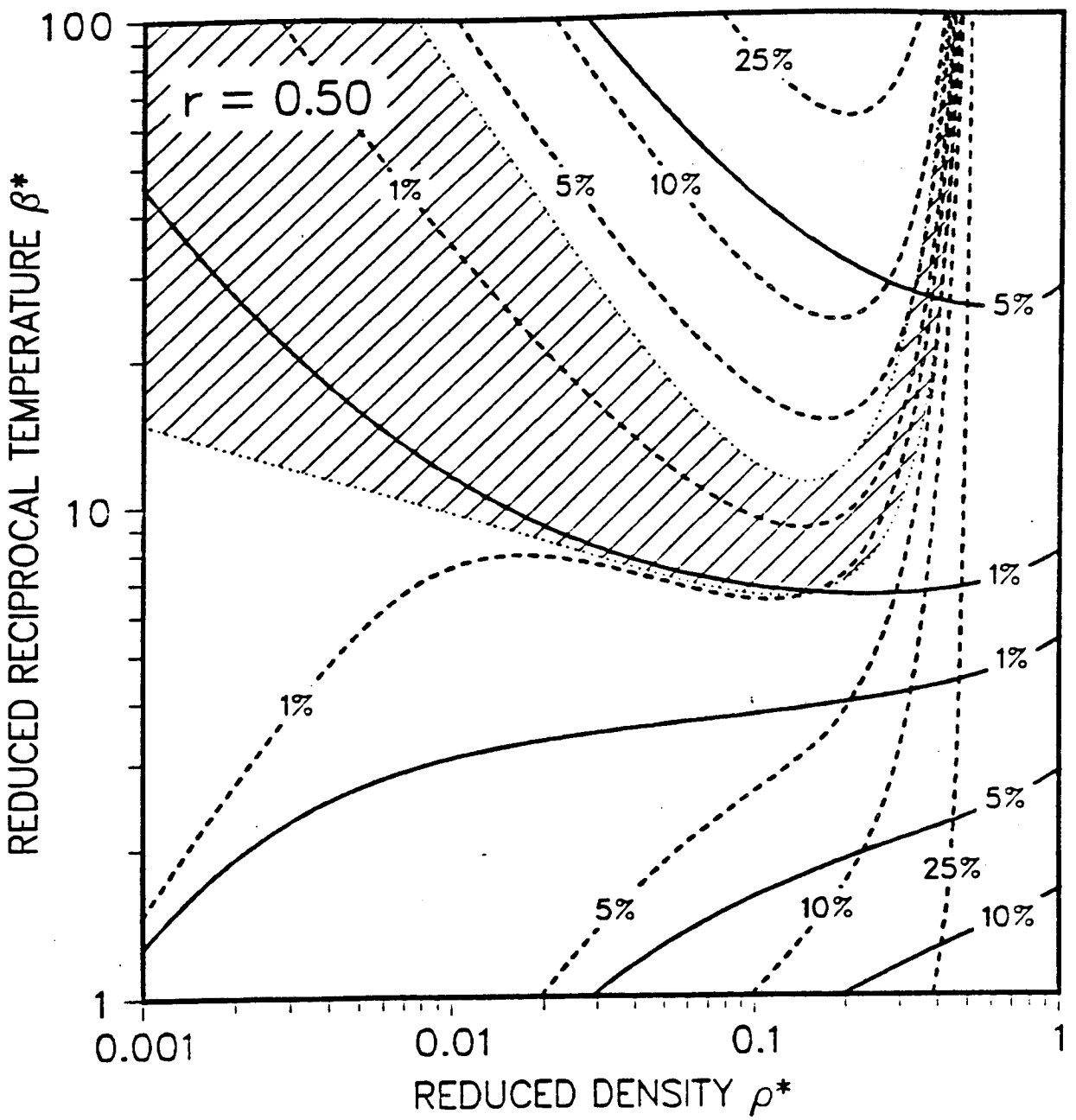

Figure 3: Contour Plot for Deviation from Full MSA Results for μ_+^{*ex} at r = 0.50. Lines and Shading as in Figure 1.

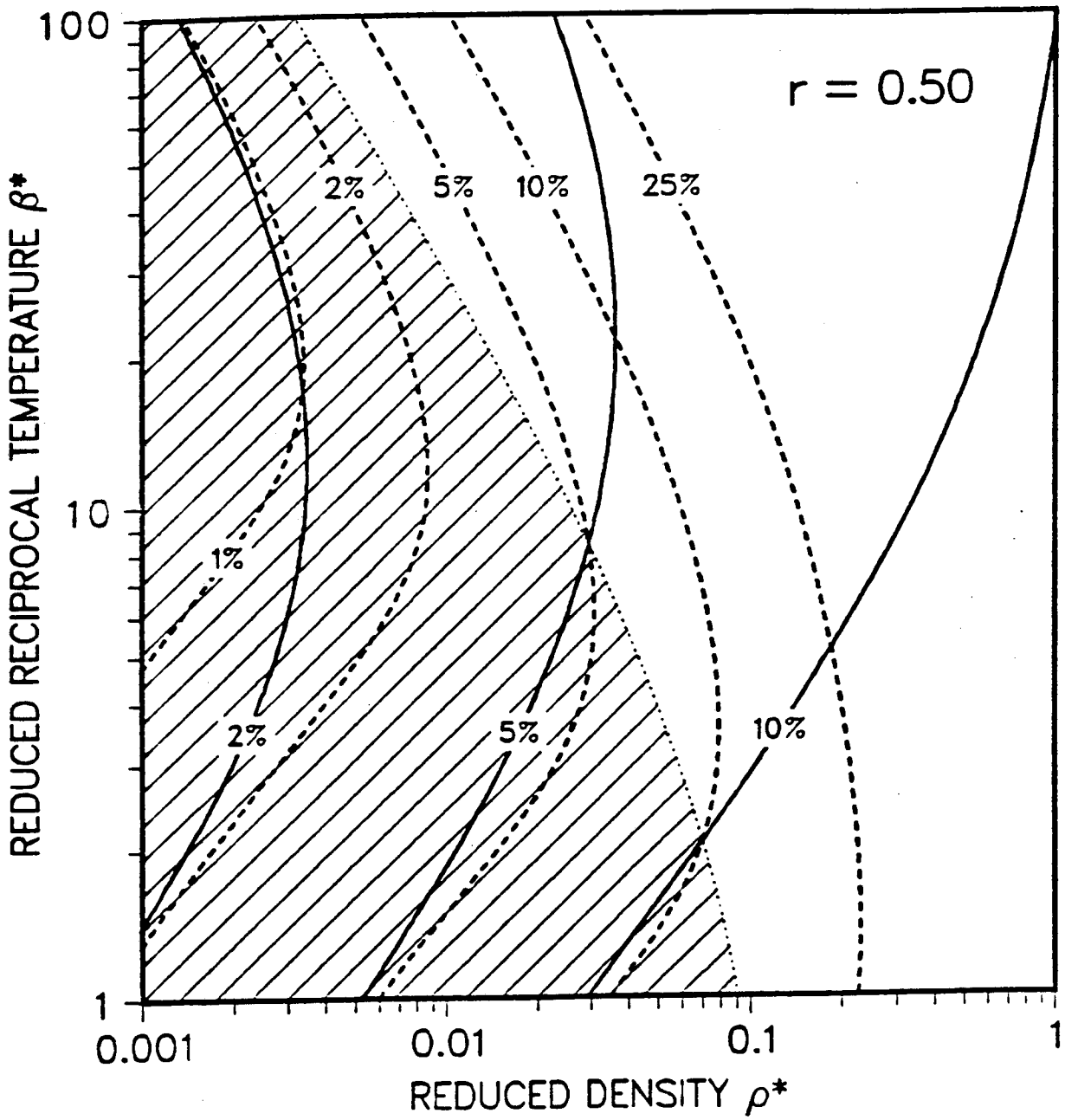

Figure 4: Contour Plot for Deviation from Full MSA Results for μ_-^{*ex} at r = 0.50. Lines and Shading as in Figure 1.

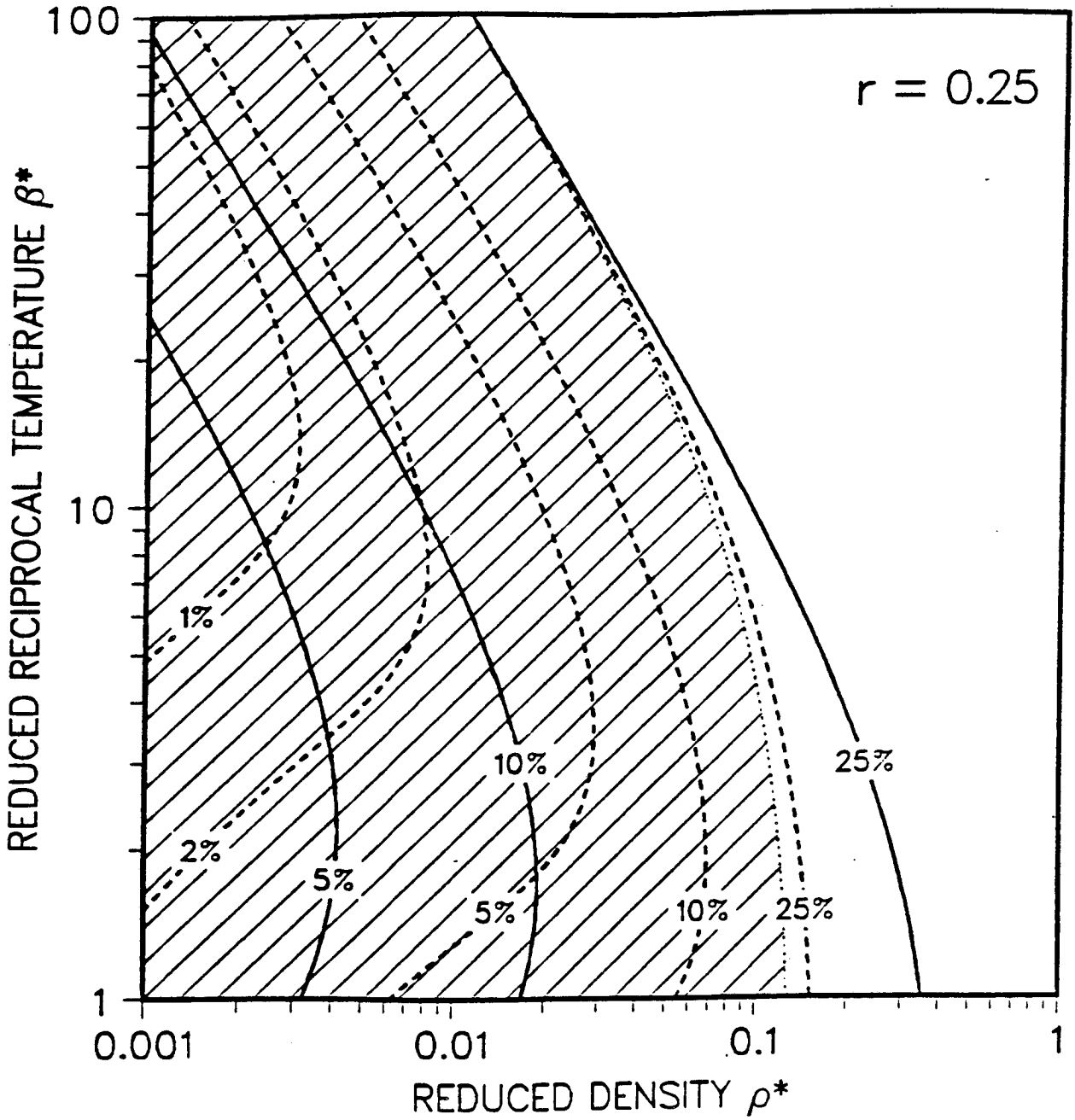

Figure 5: Contour Plot for Deviation from Full MSA Results for ϕ^{ex} at r = 0.25. Lines and Shading as in Figure 1.

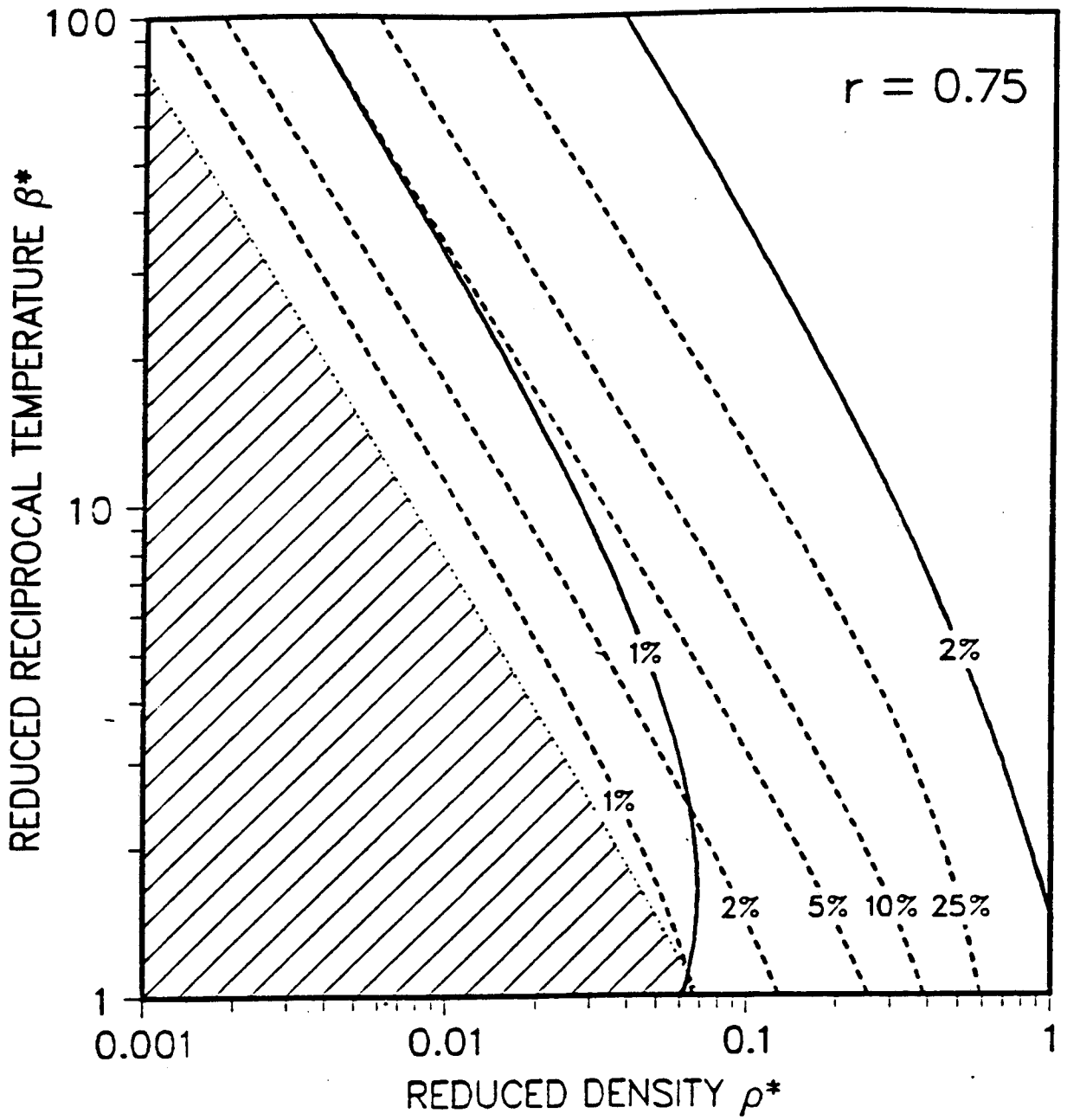

Figure 6: Contour Plot for Deviation from Full MSA Results for ϕ^{ex} at r = 0.75. Lines and Shading as in Figure 1.

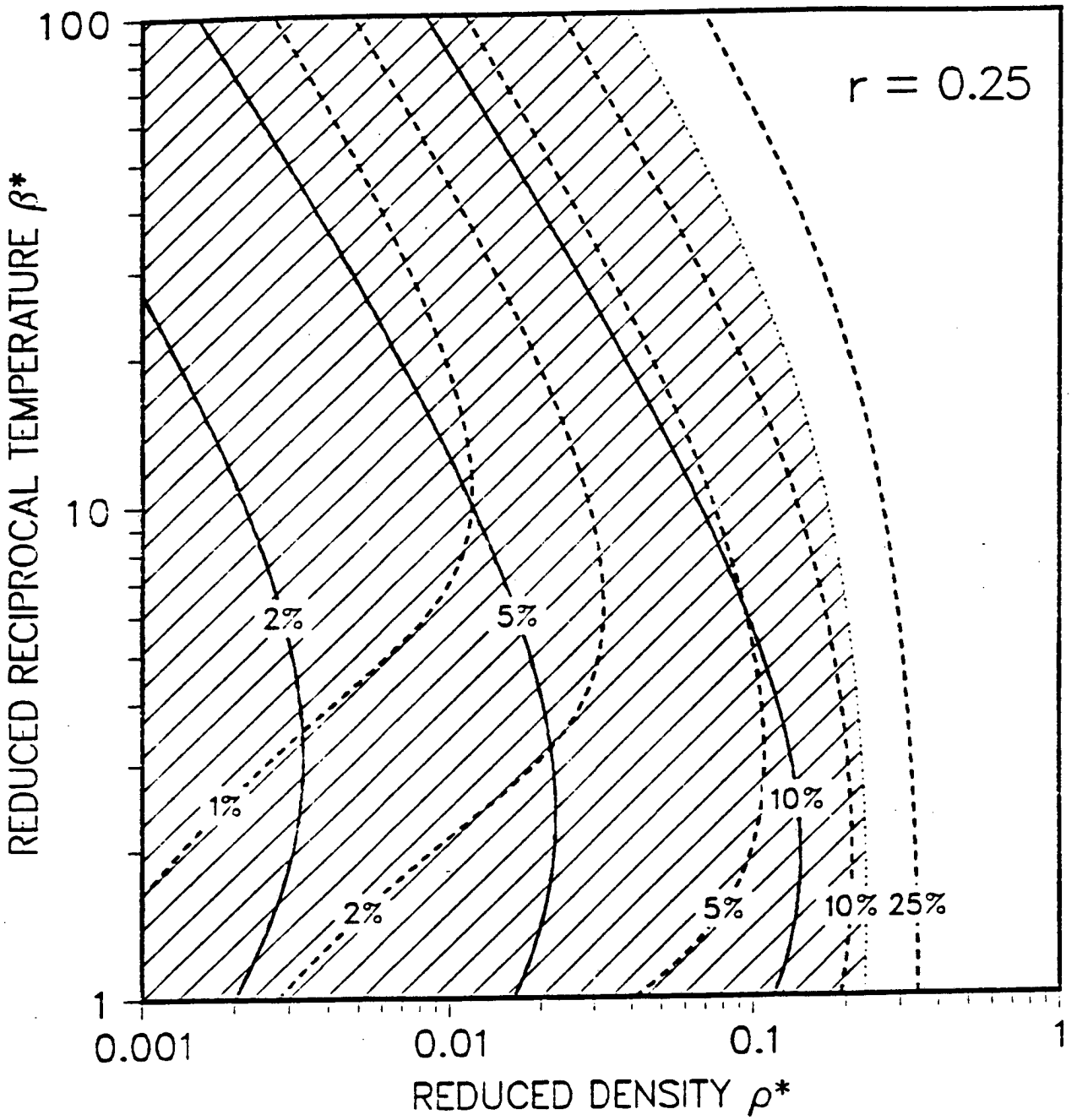

Figure 7: Contour Plot for Deviation from Full MSA Results for A^{*ex} at r = 0.25. Lines and Shading as in Figure 1.

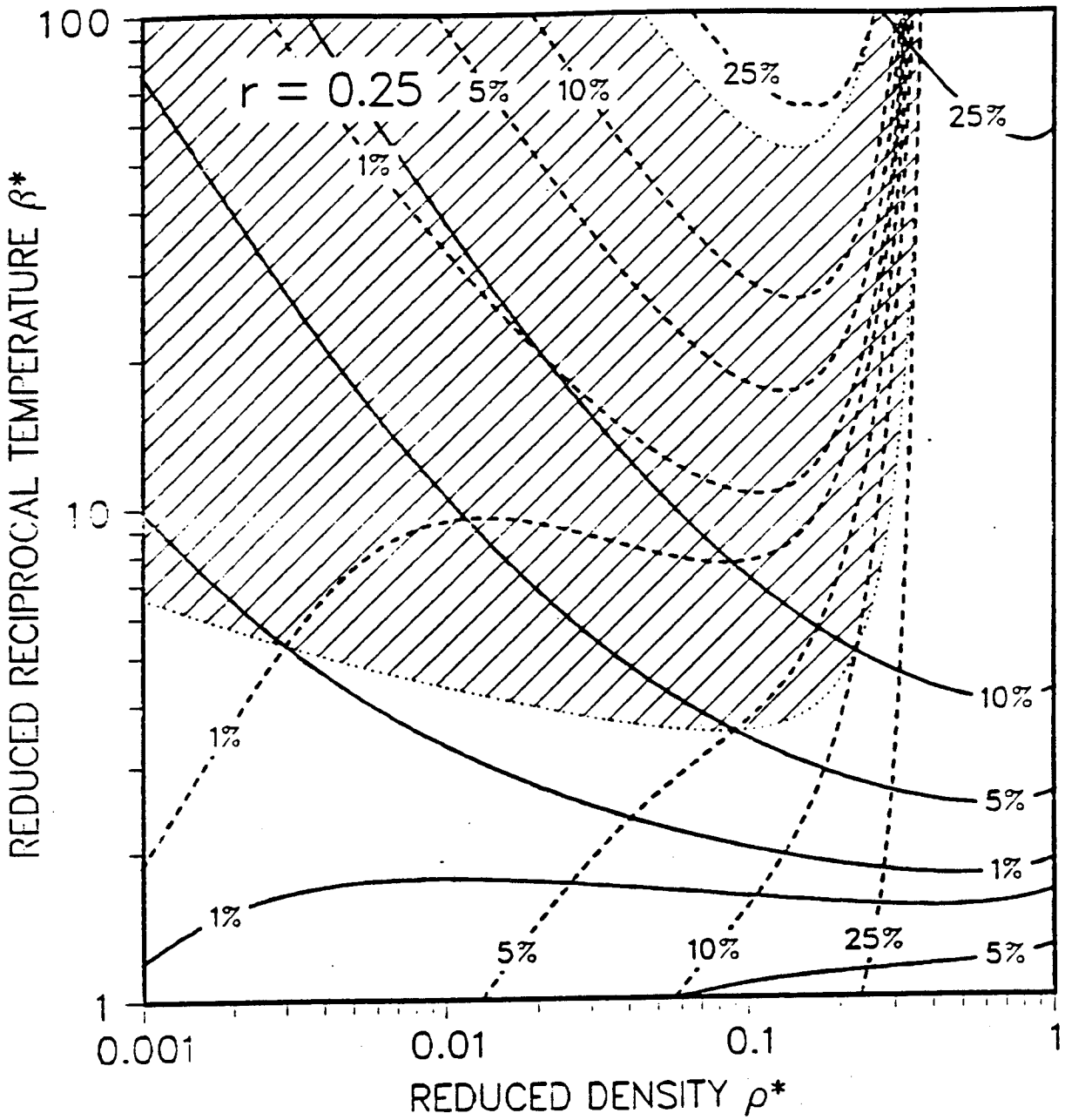

Figure 8: Contour Plot for Deviation from Full MSA Results for μ_+^{*ex} at r = 0.25. Lines and Shading as in Figure 1.

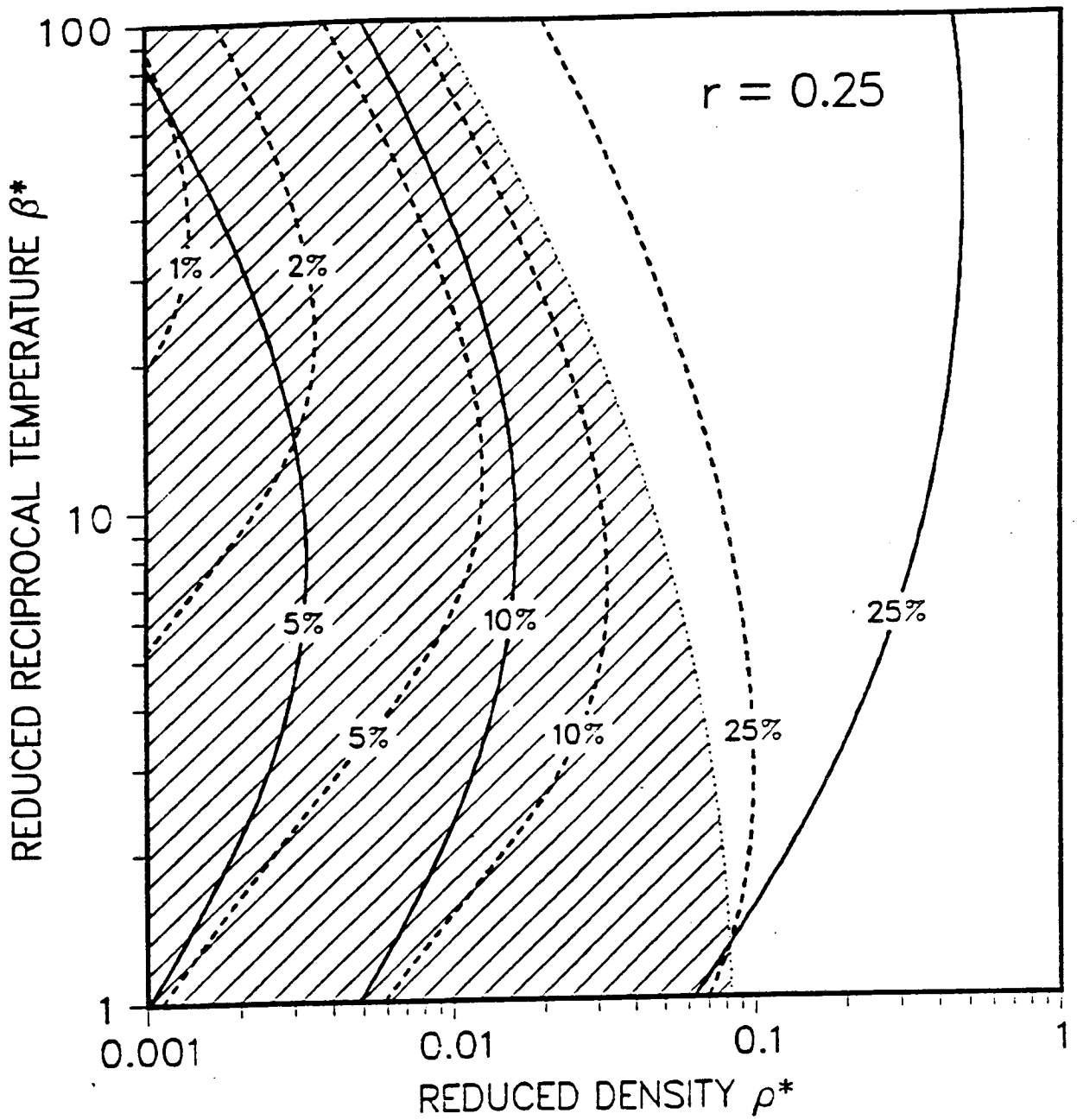

Figure 9: Contour Plot for Deviation from Full MSA Results for μ_-^{*ex} at r = 0.25. Lines and Shading as in Figure 1.

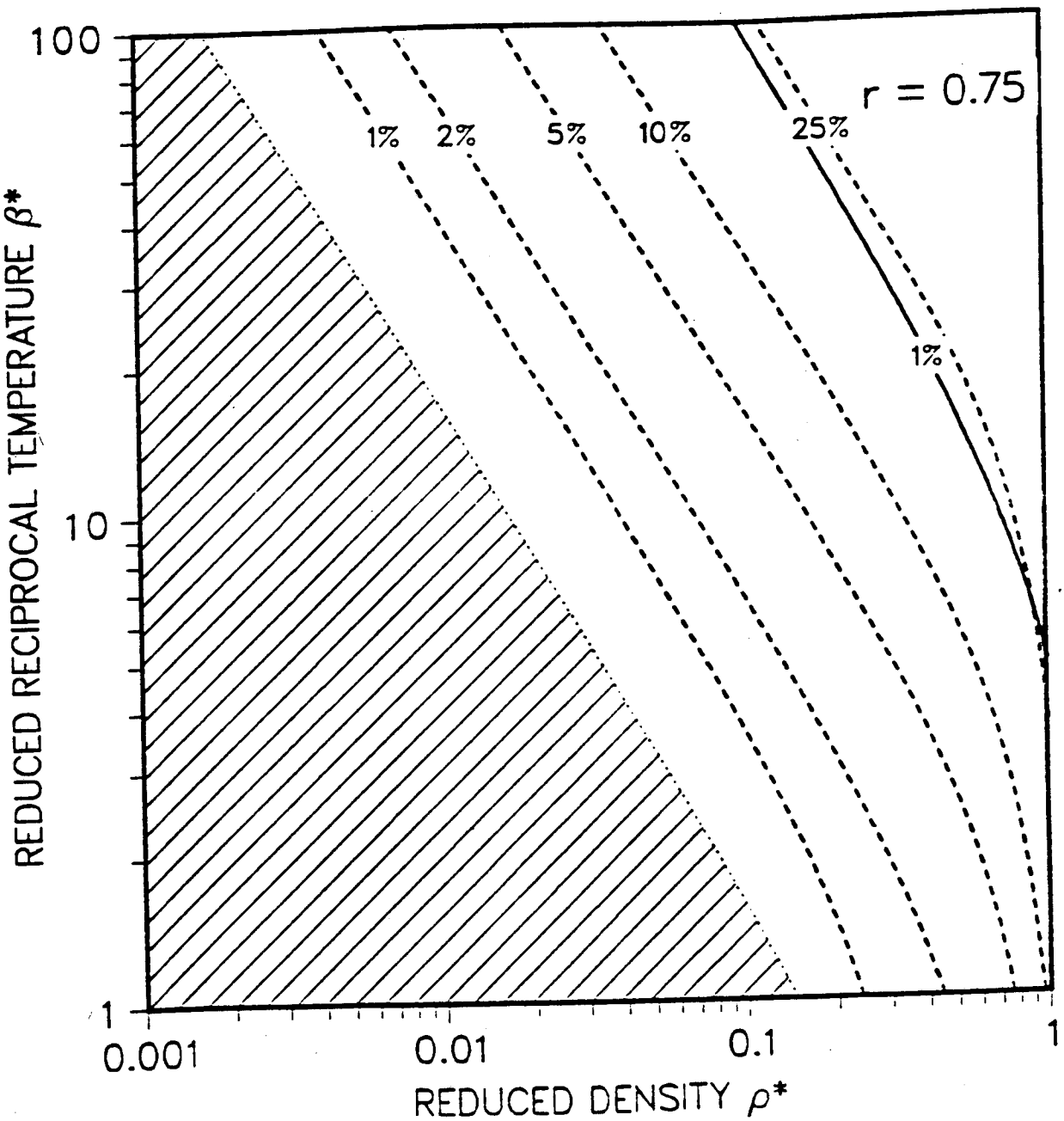

Figure 10: Contour Plot for Deviation from Full MSA Results for A^{*ex} at r = 0.75. Lines and Shading as in Figure 1.

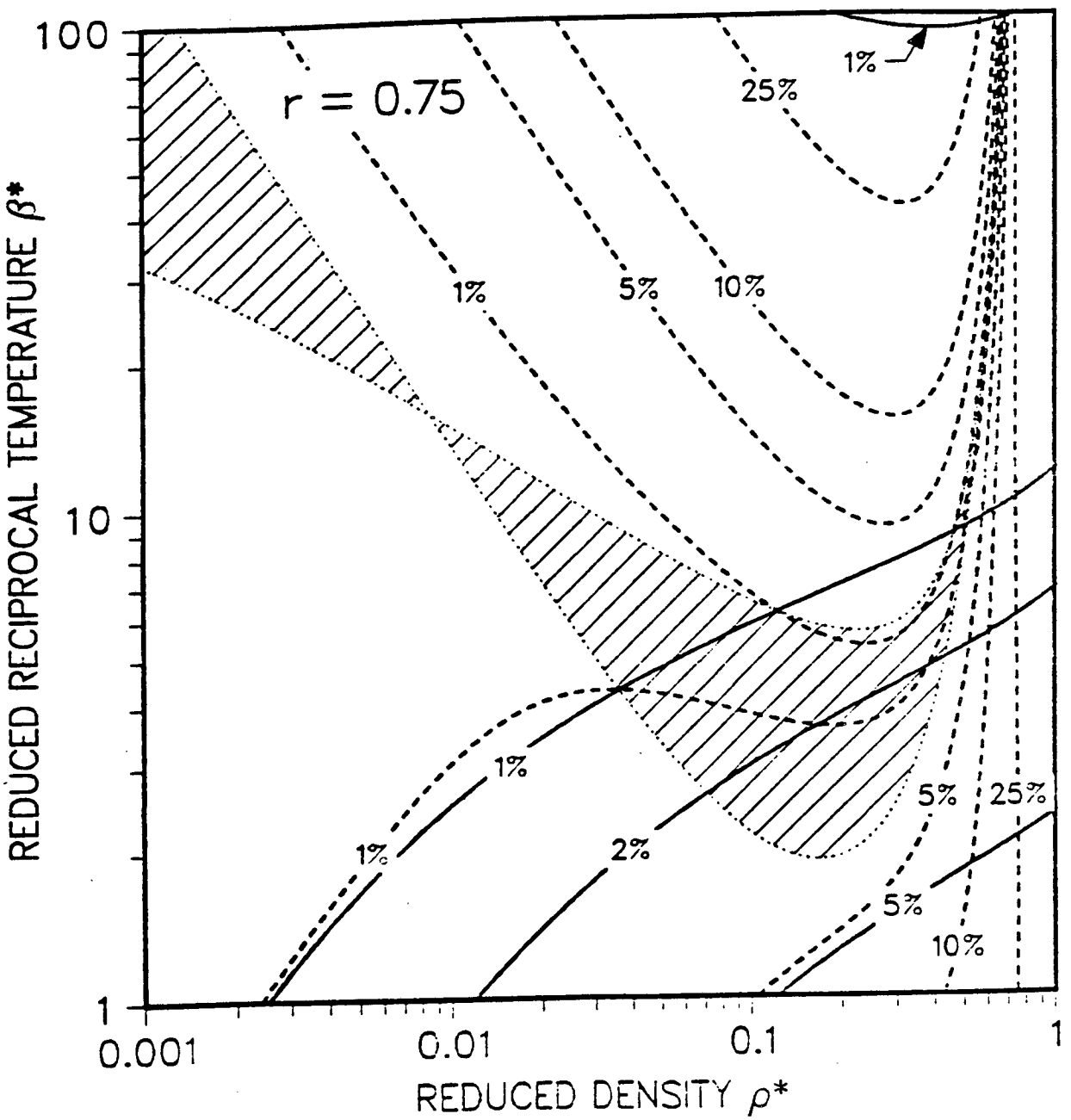

Figure 11: Contour Plot for Deviation from Full MSA Results for μ_+^{*ex} at r = 0.75. Lines and Shading as in Figure 1.

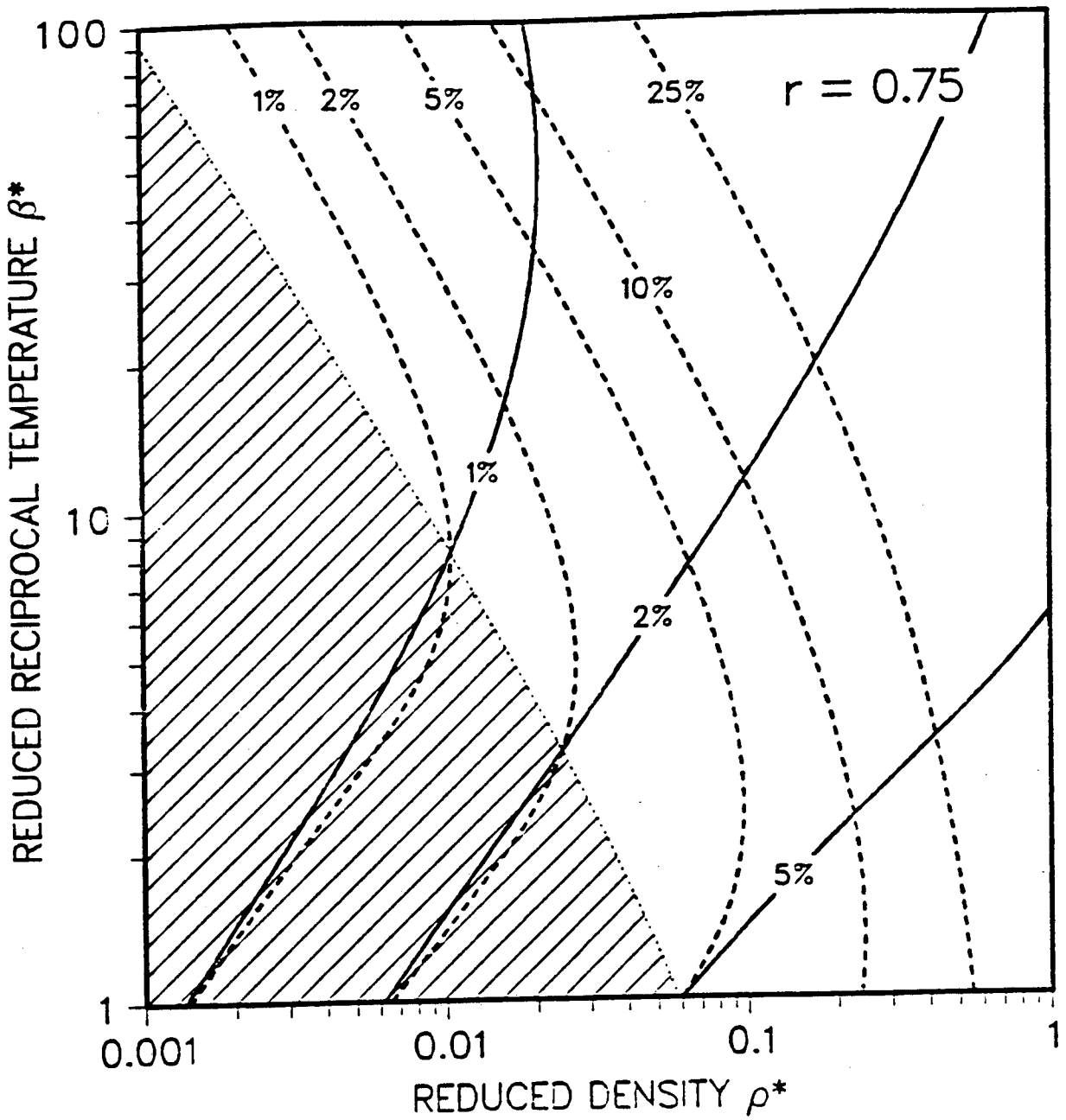

Figure 12: Contour Plot for Deviation from Full MSA Results for μ_-^{*ex} at r = 0.75. Lines and Shading as in Figure 1.

LAWRENCE BERKELEY LABORATORY
TECHNICAL INFORMATION DEPARTMENT
UNIVERSITY OF CALIFORNIA
BERKELEY, CALIFORNIA 94720